Active and Passive Elec. Comp., 1993, Vol. 15, pp. 193–210
Reprints available directly from the publisher
Photocopying permitted by license only

Printed in Malaysia

PINNING IN HIGH-T_c SUPERCONDUCTORS

ERNST HELMUT BRANDT

Max-Planck-Institut für Metallforschung, Institut für Physik Heisenbergstr. 1, W-7000 Stuttgart 80, FRG

(*Received November 15, 1992; in final form December 16, 1992*)

Magnetic flux can penetrate a type-II superconductor in the form of flux-lines or Abrikosov vortices, each of which carry a quantum of flux and arrange in a more or less regular triangular lattice. Under the action of an electric current, these flux lines move and dissipate energy unless they are pinned by material inhomogeneities. In conventional superconductors, depinning occurs when a critical current density J_c is exceeded. In high-T_c superconductors (HTSC), thermally activated depinning causes a finite resistivity ρ even at current densities $J \ll J_c$. At sufficiently large temperature T, linear (ohmic) resistivity is observed down to $J \to 0$. This indicates that the flux lines are in a "liquid state" with no shear stiffness and with small depinning energy. At lower T, $\rho(J)$ is highly nonlinear, since the pinning energy increases with decreasing J. In highly anisotropic Bi- and Tl-based HTSC, thermal depinning occurs at rather low T, since short vortex segments ("pancake vortices" in the CuO layers) can depin individually with very small activation energy.

1. THE FLUX-LINE LATTICE

Superconductivity of metals was discovered in 1911 in Leiden by Kamerlingh-Onnes after he had succeeded in liquefying helium. This puzzling phenomenon found its microscopic explanation only in 1957 by Bardeen, Cooper, and Schrieffer (BCS). But long before that date several successful *phenomenological* theories of superconductivity were known. The electromagnetic theory conceived by Fritz and Heinz London in 1935 explained the expulsion of magnetic flux from superconductors (the Meissner-Ochsenfeld effect) and introduced a magnetic penetration depth λ. The observed temperature dependence of this length, $\lambda(T) \propto (1 - T^4/T_c^4)^{-1/2}$, where T_c is the superconducting transition temperature, was explained by Gorter's two-fluid theory. The London equation states a direct proportionality of the supercurrent density $\mathbf{J}(\mathbf{r})$ and the vector potential $\mathbf{A}(\mathbf{r})$ in the "London gauge" (div$\mathbf{A}$ = 0, $\mathbf{A}$ parallel to all surfaces): $\mathbf{J} = -(\mu_0\lambda^2)^{-1}\mathbf{A}$, or λ^2rot rot $\mathbf{B} + \mathbf{B} = 0$ where $\mathbf{J} = \text{rot}\mathbf{H}$ and $\mathbf{B} = \mu_0\mathbf{H} = \text{rot}\mathbf{A}$. Pippard extended the London equation to a nonlocal relationship. The range ξ_p of the Pippard kernel was later found close to the BCS coherence length ξ_0. The Pippard theory is useful mainly in the context of type-I superconductors (with large coherence length, e.g., Sn, Pb), which are less important for application in high magnetic fields.

The most successful phenomenological theory was established in 1950 by Ginzburg and Landau (GL) from very general principles of second order phase transitions and the gauge invariance of the complex GL order parameter (or GL

function) $\Psi(\mathbf{r}) = |\Psi| \exp(i\phi)$. In the GL theory, B varies over the GL penetration length $\lambda(T)$ and Ψ over the GL coherence length $\xi(T)$. Both lengths diverge near T_c as $\lambda \propto \xi \propto (T_c - T)^{-1/2}$. The ratio $\lambda/\xi = \kappa$ is the GL parameter. GL showed that the type of solutions qualitatively differs for $\kappa < 1/\sqrt{2}$ (type-I superconductors, wall energy between normal and superconducting domains is positive) and $\kappa = 1/\sqrt{2}$ (type-II superconductors, wall energy negative, e.g., Nb and most alloys and non-metallic superconductors). Though originally derived for temperatures $T \approx T_c$, the GL theory in many cases gives qualitatively correct results valid at all temperatures $0 < T < T_c$[1-3].

In 1953, Abrikosov discovered the existence of a two-dimensional (2D) periodic solution of the linearized GL equations if $\kappa \geq 1/\sqrt{2}$. He interpreted this state as a regular lattice of current vortices, each carrying a quantum of magnetic flux $\Phi_0 = h/2e = 2.07 \times 10^{-15}\text{Tm}^2$ (Fig. 1). Abrikosov vortices are also called fluxons, fluxoids, flux tubes, flux lines, or vortex lines. The vortex positions in this flux-line lattice (FLL) are defined by the zeros of ψ. In 1957 Abrikosov published this finding [4] after similar vortices had been observed in superfluid helium. In 1967, Träuble and Essmann observed the FLL in an electron microscope by a Bitter decoration technique using iron microcrystalites that condensed from an evaporating wire in a helium atmosphere of a few Torr pressure ("magnetic smoke")[5-7]. After the discovery of high-T_c superconductors (HTSC)[8-9] similar decoration experiments also proved the existence of an Abrikosov FLL in these materials[10-11].

When the applied magnetic field B_a is increased from zero, flux lines start to penetrate an ideal (pin-free) type-II superconductor when B_a equals the lower critical field $B_{c1}(T) = (\Phi_0/4\pi\lambda^2)(\ln\kappa + \alpha)(\alpha \approx 0.5$ for $\kappa \gg 1$, $\alpha = 1 - \ln\sqrt{2} = 0.653$ at $\kappa = 1/\sqrt{2})$. The flux lines form a periodic triangular lattice of spacing $a = (\sqrt{3}\Phi_0/2B)^{1/2}$ (B = flux density), which becomes denser until superconductivity disappears at the upper critical field $B_{c2}(T) = \Phi_0/2\pi\xi^2$ where $a = 2.69\xi(T)$ and

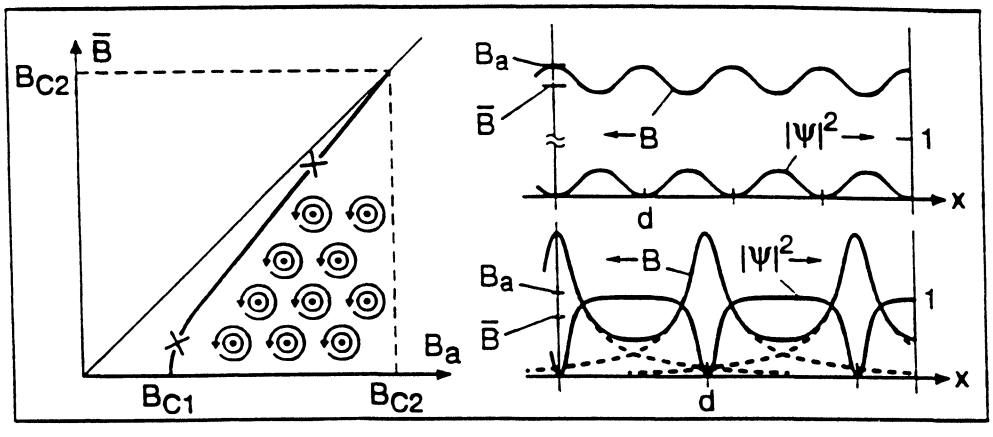

FIGURE 1 The flux-line lattice in type II superconductors: *Left*: Internal versus external magnetic field. *Right*: Profiles of magnetic field B and order parameter $|\Psi|^2$ at large (*top*) and small (*bottom*) applied fields B_a, corresponding to the two crosses in the curve $\bar{B}(B_a)$ at left. The FLL is shown schematically in the insert.

$B_a = B = B_{c2}$. The order parameter $|\Psi|^2$ is nearly constant except in the vortex core where it goes to zero in a tube of radius $r_c \approx \sqrt{2}\xi$. Its spatial average is $\langle|\Psi|^2\rangle \approx 1 - b$ with $b = B/B_{c2}$. For $\kappa > 2$ and $B > 4B_{c1}$ and zero demagnetizing effects (long specimen in parallel field) one has a very small *reversible* magnetization, $-M = B_a - B \approx (B_{c2} - B)/2\kappa^2 \ll B$.

For $\kappa > 2$ and $B < 0.25B_{c2}$ the local magnetic field $B(\mathbf{r})$ of an arbitrary arrangement of straight parallel vortices is the linear superposition of isolated vortex fields $B_v(r)$; the logarithmic divergence of the London $B_v(r)$ at the vortex center $r = 0$ is rounded over the GL vortex core radius, $B_v(r) \approx (\Phi_0/2\pi\lambda^2)K_0[(r^2 + 2\xi^2)^{1/2}/\lambda]$[12] where $K_0(x)$ is a modified Bessel function. The free energy of the system is the sum over the (repulsive) pairwise iteration of all vortices $V = \Phi_0 B_v(|\mathbf{r}_\mu - \mathbf{r}_\nu|)/\mu_0$, where $\mathbf{r}_\mu$, $\mathbf{r}_\nu$ are the two-dimensional (2D) vortex positions. When the vortices are curved, pairs of vortex line elements at 3D positions $\mathbf{r}_\mu$, $\mathbf{r}_\nu$ interact by a vectorial (non-scalar) potential $V = [\Phi_0^2 \exp(-r/\lambda')/(8\pi\mu_0\lambda'^2 r)]d\mathbf{r}_\mu \cdot d\mathbf{r}_\nu$[13] where $r = |\mathbf{r}_\mu - \mathbf{r}_\nu|$. The total energy of the vortex arrangement is obtained by integrating this potential along the flux lines and summing over all vortex pairs. These transparent London results, valid for $b < 0.25$, can be extended to higher inductions[13] by means of the GL theory. This increases the range of the magnetic repulsion $\lambda \to \lambda' = \lambda/\langle|\Psi|^2\rangle^{1/2} \approx \lambda/(1 - b)^{1/2}$ and adds and attractive "condensation energy term" of range $\xi' = \xi/(2 - 2b)^{1/2}$ that originates from the overlap of the vortex cores. If the displacements of the flux lines from their equilibrium positions are small (more precisely, if the strains of the FLL are $\ll 1$), one may apply the elasticity theory of the FLL derived from GL theory in [14].

If the pinning centres are small and placed in random distribution, the vortex lattice can be taken as an elastic continuum and the distance of a pinning centre to a given flux line is small, then the total pinning fore can be calculated assuming a static, friction-type force, characterizing the vortex-pinning interaction. In this case the resulting total pinning force does not show a threshold criterion[15]. The transition point where the quadratic dependence of the total pinning force on the individual pinning forces goes over into a linear one can be determined in agreement with experimental results for type II superconductors of low GL-parameter.

2. HIGH-T_c SUPERCONDUCTORS

Besides having higher transition temperatures T_c, HTSC differ from conventional superconductors by their short coherence length and by their pronounced anisotropy. In the following, only monocrystalline (not ceramic) HTSC will be considered. The ratio of the London penetration depth for currents flowing along the c-axis and along the a- and b-axes in the (almost) uniaxial $YBa_2Cu_3O_7$ (YBCO) superconductor is $\lambda_c/\lambda_{ab} \approx 5$, and much larger ($\geq 60$) in Bi- and Tl-based HTSC. This anisotropy can be extracted from torque measurements[16]. In anisotropic superconductors for certain directions of the applied field the vortices can attract each other[17] and may form chains. Such chains have been observed in decoration experiments[18]; it is not yet fully understood why the chains coexist with a FLL as it is seen in [18]. The energy of arbitrary arrangements of vortices in anisotropic London superconductors is given in [19–21] and the corresponding linear elastic energy in [22–24].

If the coherence length along the c-axis, $\xi_c = \xi_{ab}\lambda_{ab}/\lambda_c \ll \xi_{ab}$, is shorter than the spacing s between the CuO planes, then these planes may be considered as superconducting layers that interact only weakly with each other. This case is realized in Bi and Tl HTSC, provided T is not extremely close to T_c, where $\xi \propto (T_c - T)^{-1/2}$ diverges and thus eventually will exceed s. An elegant and very useful theory of layered superconductors is the Lawrence-Doniach (LD) theory[25-26], which describes each layer by a 2D GL parameter $\Psi_n(x,y)$ and replaces the gradient along z by a finite difference. The LD model can be derived from a tight-binding formulation of the BCS-theory[26]. With decreasing coupling between the layers, it yields first the anisotropic GL theory or the London theory when $B \ll B_{c2}$ and thus $|\Psi_n| \approx const.\ \exp[i\phi_n(\mathbf{r})]$, then the case of weakly coupled layers, and finally completely separated layers with no current flowing along the c-axis, complete transparency for the in-layer component of B, and only *magnetic* interaction between the vortices in the layers. Two novel types of vortices occur in layered HTSC:

(a) A vortex line threading the layers is composed of *point vortices* in the CuO planes[27-29], Fig. 2. If these point vortices are perfectly aligned, the usual FLL results. But pinning and thermal fluctuations may disorder the vortex dots such that one cannot draw a unique vortex line through their centers. The spatial variation of the magnetic field $\sigma^2 = \langle[\mathbf{B}(\mathbf{r}) - \langle\mathbf{B}(\mathbf{r})\rangle]^2\rangle$ is then drastically reduced[30]. One has $\sigma = \sigma_0 = 0.061\Phi_0/\lambda^2$ for a perfect FLL with $2B_{c1} < B \ll B_{c2}$; $\sigma^2 = B\Phi_0/4\pi\lambda^2$ for randomly positioned parallel flux lines; $\sigma^2 = B\Phi_0 s/8\pi\lambda^3$ for a random arrangement of point vortices (s = layer spacing); and $\sigma^2 = (1.5s/a)\sigma_0^2 \ll \sigma_0^2$ for nearly perfect vortex-point lattices in the layers that are randomly displaced with respect to each other. These vortex dots or "pancake vortices"[31] interact by their magnetic field

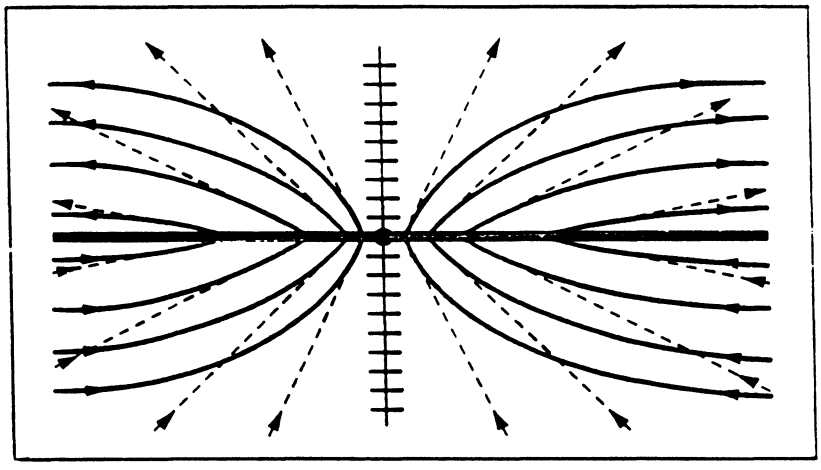

FIGURE 2 The magnetic field lines of a point vortex or pancake vortex (thick lines) in a superconductor consisting of almost isolated superconducting layers indicated by the dashes near the z-axis (the crystalline c-axis). Compared to the field lines of a point vortex in a thin film (dashed lines), the field lines in a layered structure curve such that they become *parallel* to the layers at large distances from the vortex core. Their field is thus confined to a disk of thickness $\approx 2\lambda_{ab}$.

and by the phase difference of the order parameter in adjacent layers. The latter interaction, $\propto 1 - \cos(\phi_{n+1} - \phi_n)$, is called Josephson coupling and leads to a tunneling current between the layers $\propto \sin(\phi_{n+1} - \phi_n)$. Point vortices in the same layer repel, and in different layers attract each other such that the ground state is a regular lattice of parallel vortex lines. The magnetic interaction between the points is logarithmic up to very large distances, since the magnetic field of each point vortex is confined to a layer of thickness $2\lambda_{ab}$. In contrast, the field of a point vortex in a *single* layer or thin film is radially outgoing above, and radially incoming below the film and the interaction is logarithmic only for distances smaller than the penetration depth of the film, $\lambda_{film} = 2\lambda^2/d$ (d = film thickness).

(b) When the applied field B_a is almost parallel to the layers, the vortex cores prefer to lie between the superconducting layers[32]. This phenomenon is called intrinsic pinning, since here, pinning is not caused by structural defects but by a perfect crystal lattice. If the Josephson coupling is weak, then the current circulating around a vortex core has to tunnel from one layer to the next. Such a "Josephson vortex" has no vortex core in the usual sense (tube of compressed order parameter), since within the LD theory the order parameter is not defined between the layers. When B_a is not exactly parallel to the layers, the flux lines form kinks (Fig. 3) composed of point vortices and Josephson vortices. A "lock-in transition" may occur when the orientation of B_a is changed and comes close to the ab-plane; the vortex kinks then straighten and B becomes exactly parallel to the layers[28–29].

If the thermal energy k_BT exceeds the coupling energy between the vortices in adjacent layers, the two-dimensional (2D) vortex lattices in each CuO layer decouple and may melt like a 2D lattice[27]. A single vortex line thus "evaporates" into independent point vortices[31] at the same temperature T_{KT}, where a vortex-antivortex pair in a single layer dissociates in zero field (Kosterlitz-Thouless transition), $k_BT_{KT} = \Phi_0^2 s/8\pi\mu_0\lambda_{ab}^2$. Furthermore, vortex lines may nucleate sponta-

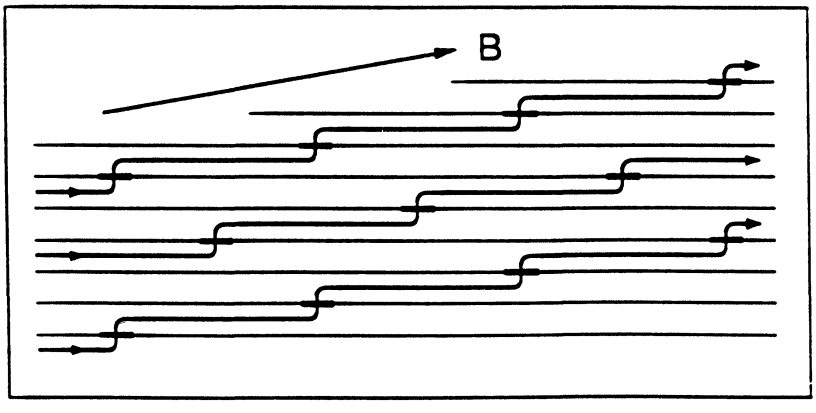

FIGURE 3 The flux lines form kinks when the applied field is at a small angle with respect to the superconducting CuO planes. Such vortex kinks consist of point vortices in the layers and pieces of Josephson vortices between the layers.

neously above the temperature T = U/S, where their free energy F = U − TS turns negative due to the entropy S of their thermal fluctuations[33,34].

3. FLUX FLOW AND PINNING

An electric current density **J** exerts a Lorentz force density **B** × **J** on the flux-line lattice, which causes the vortices to move with mean velocity **v**. This vortex drift dissipates energy and thus generates an electric field **E** = **B** × **v**, where **B** is the flux density or magnetic induction in the sample. The dissipation is caused by two effects that give approximately equal contributions: (a) by dipolar currents that surround each moving flux line (eddy currents) and have to pass through the normal conducting vortex core[35]; (b) by the retarded relaxation of the order parameter $\Psi(\mathbf{r})$ when the vortex core moves[36]. Since at low B the dissipation of the vortices is additive, and since at the upper critical field $B_{c2}(T)$ the flux-flow resistivity ρ_{FF} has to reach the normal conductivity ρ_n, one approximately gets $\rho_{FF} \approx \rho_n B/B_{c2}(T)$. A more quantitative treatment of this flux dissipation uses time-dependent Ginzburg-Landau theory. For reviews of flux motion see [37–38], and for extensions to layered and anisotropic superconductors [39–41]. See also the overview by Clem [42].

In real superconductors at small current densities $J < J_c$, the flux lines are pinned by inhomogeneities in the material, e.g., by dislocations, vacancies, interstitials, grain boundaries, precipitates, or by a rough surface, Fig. 4. Only when J exceeds a critical value J_c do the vortices move and dissipate energy[43]. Pinning of flux lines has two important consequences:

(a) The current-voltage curve of a superconductor in a magnetic field is highly nonlinear, with E = 0 for $J < J_c$ and $E = \rho_{FF}J$ for $J \gg J_c$. For J slightly above J_c,

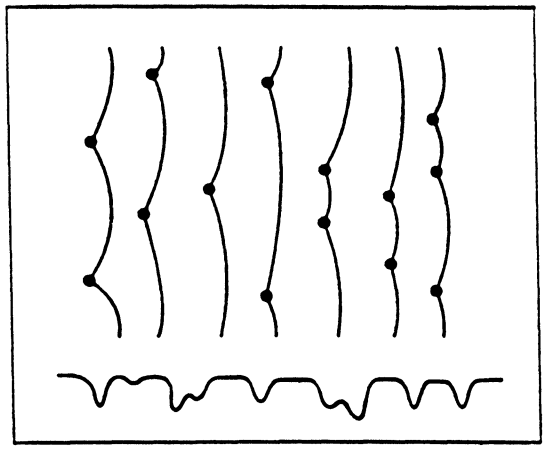

FIGURE 4 *Top*: Flux lines pinned by point pins, e.g., oxygen vacancy clusters. The Lorentz force acts to the right. *Bottom*: Random pinning potential.

various shapes of E(J) are observed, depending on the type of pinning and on the geometry of the sample. Often

$$E(J) = 2\rho_{FF}[1 - (J_c/J)^p]^{1/p} \qquad (J \geq J_c) \tag{1}$$

is a good approximation with, e.g., p = 1 or p = 2.

(b) The magnetization curve $M(B_a)$ exhibits a hysteresis, Fig. 5. When B_a is increased or decreased the magnetic flux enters or exits until a *critical slope* is reached (like in a pile of sand), namely, a maximum and nearly constant gradient of $B = |\mathbf{B}|$, Fig. 5. More precisely, in this *critical state* the *current density* reaches a maximum value J_c; one has $\mathbf{J} = (\partial H/\partial B)\nabla \times \mathbf{B} \approx \mu_0^{-1}\nabla \times \mathbf{B}$, where $H(B) \approx B/\mu_0$ is the (reversible) magnetic field that would be in equilibrium with the induction **B**. The critical state is often well described by the "Bean model"[44], which assumes a B-independent J_c and disregards demagnetizing effects; these become important in flat superconductors in perpendicular magnetic field[45–49].

In general, the current density in type-II superconductors may have three different origins: (a) surface currents within the penetration depth λ; (b) a *gradient* of the flux-line density; or (c) a *curvature* of the flux lines (or field lines). The latter two contributions are easily seen by writing $\nabla \times \mathbf{B} = \nabla B \times \hat{\mathbf{B}} + B\nabla \times \hat{\mathbf{B}}$ where $\hat{\mathbf{B}} = \mathbf{B}/B$. In bulk samples typically the gradient term dominates, $J \approx \mu_0^{-1}\nabla B$, but in films the current is carried almost entirely by the *curvature* of the flux lines[45–49].

4. THERMALLY ACTIVATED FLUX MOTION

As predicted in 1962 by Anderson[43], thermally activated depinning of the flux lines may occur at finite temperatures T. In conventional superconductors this effect is

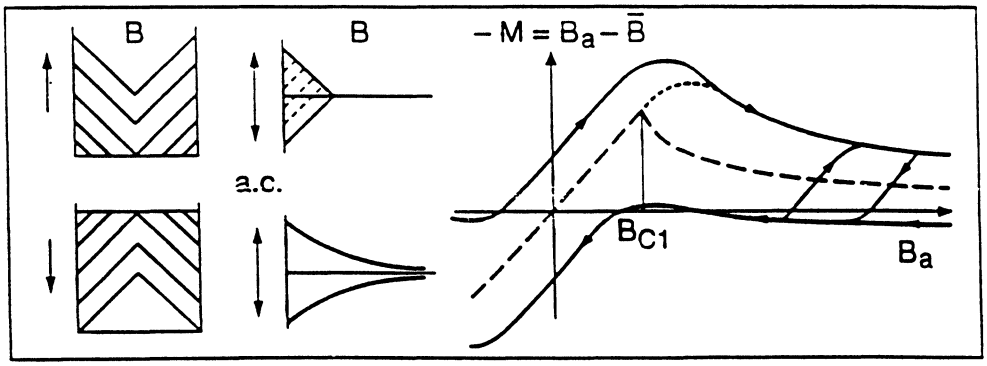

FIGURE 5 Field profiles in a superconducting cylinder or slab with strong pinning in increasing (*left top*) and decreasing (*left bottom*) applied field. In this Bean model the field gradient is constant. Also shown is the field profile caused by an additional weak a.c. field near the surface in the Bean model (*middle, top*) and in the cases of elastic pinning, viscous drag, or thermally assisted flux flow (*middle, bottom*). Strong pinning leads to hysteretic magnetization curves (*right*) with the irreversible magnetization (solid lines) lying above and below the ideal reversible curve (dashed line).

observed only close to the transition temperature T_c as *flux creep*[50]. Flux creep occurs in the critical state after the applied magnetic field is changed. The field gradient, and the persistent currents and magnetization, then slowly *decrease with a logarithmic time law*. Formally, this flux creep is equivalent to a highly nonlinear, current dependent flux-flow resistivity, e.g., $\rho \propto \exp(J/J_1)$. Initially, the persistent currents in a ring feel a large ρ, but as the current decays, ρ decreases rapidly and so does the decay rate $-\dot{J} \propto \rho \propto \exp(J/J_1)$.

In HTSC, thermal depinning is observed in a large temperature interval below T_c. This "giant flux creep"[51–53] occurs mainly because (a) the superconducting coherence length ξ ($\approx$ vortex core radius) is small, (b) the magnetic penetration depth λ is large, and (c) these materials are strongly anisotropic. All three properties decrease the pinning *energy* but tend to increase the pinning *force* as discussed below.

Small ξ means that the elementary pinning *energy* U_p of small pins, e.g., oxygen vacancies or clusters thereof is small, of the order of $(B_c^2/\mu_0)\xi^3 = (\Phi_0^2/8\pi^2\mu_0\lambda^2)\xi$. The elementary pinning *force* U_p/ξ, however, is *independent* of ξ in this estimate and is thus not necessarily small in HTSC.

Small λ means that the stiffness of the FLL with respect to shear deformation and to short-wavelength tilt is small. Therefore, the flux lines can better adjust to the randomly positioned pins. This flexibility increases the average pinning force density. (The argument that a soft FLL or a flux-line liquid with vanishing shear stiffness cannot be pinned since it may flow around the pins, does not apply to the realistic situation where there are many more pins than flux lines like in Fig. 4.) The statistical summation of pinning forces at $T = 0$[54] and $T > 0$[55–57] requires the correct (non-local) elasticity theory of the FLL[13,14,20–24]. The elasticity is non-local, i.e., stresses depend on strains within a certain distance and the elastic moduli depend on the strain wavelength since the range λ of the vortex interaction is typically much larger than the vortex spacing a.

Large material anisotropy effectively softens the FLL and *increases* the average pinning force, but it *decreases* the pinning energy. In particular, long columnar pins generated by high-energy (500 MeV) heavy ion irradiation perpendicular to the CuO planes in YBCO[58] or BSCCO[59] are most effective pins at low T if the flux lines are parallel to the pins. However, at higher T, columnar pins can pin flux lines only in YBCO, but in the very anisotropic BSCCO the flux lines easily break into short segments or point vortices that then depin individually with very small activation energy[59–61]. As a consequence, BSCCO tapes are good superconductors only at $T = 4K$. In principle, if B could be kept strictly parallel to the layers, large J_c and weak thermal depinning could be achieved even at $T = 77K$, but this geometric condition appears very difficult to satisfy.

5. THE KIM-ANDERSON THEORY

A novel feature in HTSC is that a linear (ohmic) resistivity ρ is observed at small current densities $J \ll J_c$ in the region of thermally assisted flux flow (TAFF)[52–53]. Both effects, flux creep at $J \approx J_c$ and TAFF at $J \ll J_c$, are limiting cases of

Anderson's[43] general expression for the electric field E(B, T, J) caused by thermally activated flux jumps out of pinning centers, which may be written as[62]

$$E(J) = 2\rho_c J_c \exp(-U/k_BT) \sinh(JU/J_cK_BT) \tag{2}$$

In (2), $J_c(B)$ (the critical current density at T = 0), $\rho_c(B, T)$ (the resistivity at J = J_c), and U(B, T) (the activation energy for flux jumps) are *phenomenological parameters*. The physical idea behind eqn. (2) is that the Lorentz force density **J** × **B** acting on the flux-line lattice (FLL) *increases* the rate of thermally activated jumps of flux lines or flux-line bundels along the force, $\nu_0 \exp[-(U + W)/k_BT]$, and *reduces* the jump rate for backward jumps, $\nu_0 \exp[-(U + W)/k_BT]$. Here U(B, T) is an activation energy, W = JBVl the energy gain during a jump, V the jumping volume, l the jump width, and ν_0 is an attempt frequency. All these quantities depend on the microscopic model, which is still controversial, but by defining a critical current density $J_c = JU/W = U/BVl$, only measurable quantities enter. Subtracting the two jump rates to give an effective rate ν and then writing the drift velocity $v = \nu l$ and the electric field $E = vB = \rho J$ one obtains (2).

For large currents $J \approx J_c$, one has $W \approx U \gg k_BT$ and, thus, $E \propto \exp(J/J_1)$ with $J_1 = J_ck_BT/U$. For small currents $J \ll J_1$, one may linearize the $\sinh(W/k_BT)$ in (2) and get *ohmic* behavior with a thermally activated linear resistivity $\rho_{TAFF} \propto \exp(-U/k_BT)$. Combining (2) with the usual, not activated flux-flow resistivity ρ_{FF} valid at $J \gg J_c$, or with the square-root result [p = 2 in (1)] for a particle moving viscously across a one-dimensional sinusoidal potential (see appendix in [63]), one gets (Fig. 6)

$$\rho = (2\rho_cU/k_BT) \exp(-U/k_BT) = \rho_{TAFF} \quad \text{for} \quad J \ll J_1 \text{ (TAFF)} \tag{3}$$

$$\rho = \rho_c \exp[(J/J_c - 1)U/k_BT] \propto \exp(J/J_1) \quad \text{for} \quad J \approx J_c \text{ (flux creep)} \tag{4}$$

$$\rho = \rho_{FF}(1 - J_c^2/J^2)^{1/2} \approx \rho_{FF} \approx \rho_nB/B_{c2}(T) \quad \text{for} \quad J \gg J_c \text{ (flux flow).} \tag{5}$$

The existence of the linear TAFF regime (3) is confirmed by experiments in certain regions of B and T in [64–68]. It appears today that in the TAFF regime, the FLL is in a "liquid" state[57], i.e., it has no shear stiffness; therefore, elastic deformations of the FLL at different points are not correlated. This assumption leads to an activation energy that does not depend on the current density.

6. COLLECTIVE CREEP AND VORTEX GLASS SCALING

Theories of collective pinning[55–57] going beyond Anderson's model (2) predict that the thermally jumping volume V of the FLL depends on the current density J and becomes infinitely large for $J \to 0$. As a consequence, the activation energy also diverges, e.g., $U \propto V \propto 1/J^\alpha$ with $\alpha > 0$, thus the resistivity becomes truely zero at $J \to 0$. This result follows for weak random pinning if the FLL is treated as an elastic medium. A diverging activation energy is also obtained in theories of de-

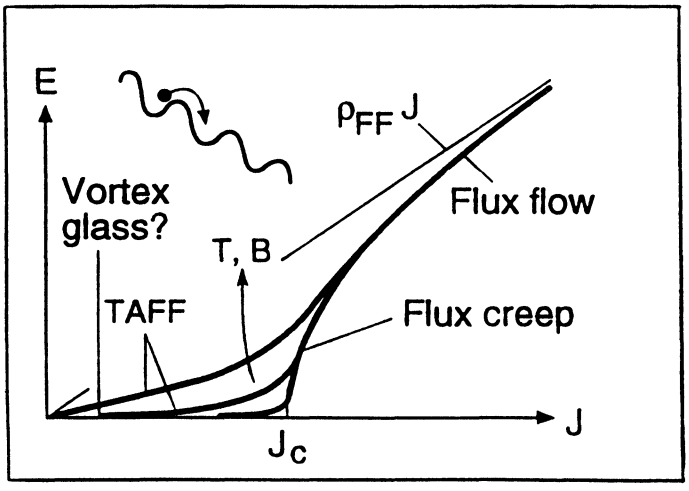

FIGURE 6 Current-voltage curves, E = electric field, J = current density, $J \gg J_c$: flux flow, $E \approx J\rho_n$; $J \approx J_c$: flux creep, $E \propto \exp(J/J_1)$; $J \ll J_c$: thermally assisted flux flow (TAFF), $E \approx J\rho_n \exp(-U/k_BT)$, or, at low T: vortex glass, $E \propto \exp(-J_2^{\varsigma}/J^{\alpha})$. Top: Tilted periodic pinning potential with jumping flux-line bundle.

pinning via a kink mechanism of vortices from the space between the CuO layers[71] and from columnar pins[60–61].

A similar result is arrived at by the "vortex glass" picture[72–73]. Its basic idea is that if there is a glass-transition temperature T_G in the vortex-pin system similar as in theories of spin glasses, then a characteristic length ξ_G (the size of the jumping volume) in the FLL should diverge as $\xi_G \propto |T - T_g|^{\nu}$ ($\nu \approx 1$) when T approaches T_G. The vortex-glass picture predicts scaling laws, e.g., the electric field should scale as $E\xi_G^{z-1} = f_{\pm}(J\xi_G^{D-1})$ where $z \approx 4$, D is the spatial dimension, and $f_{\pm}(x)$ are scaling functions for the regions above and below T_G. For $x \to 0$ one has $f_+(x) =$ constant and $f_-(x) \to \exp(-x^{-\mu})$. At T_G, a power-law current-voltage curve is expected, $E \propto J^{(z+1)/(D-1)}$, thus

$$\rho \propto J^{(z+1)/(D-1)-1} \quad \text{for} \quad T = T_G \tag{6}$$

$$\rho \propto \exp[(-J_2/J)^{\alpha}] \quad \text{for} \quad T > T_G. \tag{7}$$

In the theory of collective pinning[55] there is no explicit glass temperature, but the picture is similar since collective creep occurs only below a "melting temperature" T_m, above which the FLL loses its elastic stiffness. Thus, T_m has a similar meaning as T_G. A vortex glass state should not occur in 2D flux-line lattices[27]. More details may be found in [73–74] and in the review paper[75].

Experiments that measure the magnetization decay or the voltage drop with high sensitivity appear to confirm this scaling law in various HTSC in an appropriate range of B and T. For example, by plotting T-dependent creep rates M = dM/dt in reduced form, $(1/J)|1 - T/T_G|^{-\nu(z-1)}$ M versus $J|1 - T/T_G|^{-2\nu}$, van der Beek et al.[67] in BSCCO measured $T_G = 13.3$ K, $z = 5.8 \pm 1$, and $\nu = 1.7 \pm 0.15$. Very

detailed curves $\rho(J)$ for three YBCO samples with different pinning (without and with irradiation with protons or Au ions) are presented by Worthington et al.[69] for different fields B_α with T as parameter. In the sample with intermediate pinning, two transitions are seen in $\rho(J)$, a "melting transition" at T_m (e.g., $T_m \approx 91.5$K at $B = 0.2$ T, $J = 10^5$ Am^{-2}) and a "glass transition" at $T_m \approx 90$ K (above case) or $T_m = 84.92$ K (strong pinning sample, very sharp transition at $B = 4$ T, $J \leq 4 \times 10^5$ Am^{-2}). The FLL phase in between these two transitions is named "vortex slush."

7. CREEP RATES AND TUNNELING OF VORTICES

For the geometry of rings or cylinders, the decay of shielding currents within the Kim-Anderson model (2) can be calculated analytically for all times[76–77]. Combining measurements of current-voltage curves with highly sensitive measurements of decaying currents in rings of YBCO films (3 mm diameter, 0.1 mm width, 200 nm thickness), a large range of electric fields $E = 10^{-13}$ to 10^{-1} V/m is covered[78].

The current-dependent activation energy U(J) may be extracted from experiments by the method of Maley and Willis[79], see., e.g., [67]. The Kim-Anderson model (2) originally means an effective activation energy $\propto J_c - J$, cf. eqn. (4) and actually corresponds to a zig-zag shaped pinning potential. As shown by Beasley et al.[50], a more realistic smooth potential yields $U \propto (J_c - J)^{3/2}$. Collective creep theory yields $U \propto 1/J^\alpha$ with $\alpha > 0$ depending on B and the pinning strength. Other experiments suggest a logarithmic dependence $U \propto \ln(J_2/J)$ for which the creep rate can be calculated analytically[80]. Numerical solutions to the relaxation rates for various dependencies U(J) are given in [77]. Good fits to relaxation rates are also achieved by fitting a spectrum of activation energies[81–84]. The success of theories that assume only *one* activation energy U suggests that at given values of B, J, and T, essentially one effective U of an entire spectrum determines the physical process under consideration.

In numerous experiments, the creep rate plotted versus T appears to tend to a finite value at zero temperature. Flux creep observed at low temperatures[85] in principle may be explained by usual thermal activation from smooth shallow pinning wells[86], but it may also indicate "quantum tunneling" of vortices out of the pins[87–91]. Tunneling of vortices differs from tunneling of particles by the smallness of the inertial mass of the vortex: this means the vortex motion is overdamped; there are no oscillations or resonances. This overdamped tunneling is treated by Ivlev et al.[88] and Blatter et al.[89]. Griessen et al.[90] show that the dissipative quantum tunneling theory of Caldeira and Legget with the usual vortex viscosity η inserted reproduces the main results of [88–89]. In a recent paper, Blatter and Geshkenbein[91] give a very general theory of collective creep and (vortex-mass dominated) tunneling in anisotropic and layered superconductors.

8. FLUX DIFFUSION AND AC RESPONSE

Inserting the electric field induced by flux flow $\mathbf{E} = \mathbf{B} \times \mathbf{v} = \rho \mathbf{J}_\perp$, with $\mathbf{J}_\perp = \hat{\mathbf{B}} \times \mathbf{J} \times \hat{\mathbf{B}}$, the current density perpendicular to $\mathbf{B}$ and with $\hat{\mathbf{B}} = \mathbf{B}/B$ into the

induction law $\dot{\mathbf{B}} = \partial\mathbf{B}/\partial t = \nabla \times \mathbf{E}$, one obtains an interesting equation of motion for the induction $\mathbf{B}$ in isotropic superconductors containing a FLL:

$$\dot{\mathbf{B}} = \mu_0^{-1} \nabla \times \rho\hat{\mathbf{B}} \times \hat{\mathbf{B}} \times \nabla \times \mathbf{B}. \tag{8}$$

If $\mathbf{B}(\mathbf{r}, t) \approx const. = \mathbf{B}_0$ varies little in space and time, eqn. (8) may be linearized to give[62]

$$\dot{\mathbf{B}} = D\nabla^2\mathbf{B} + \rho\nabla \times \mathbf{J}_\parallel \tag{9}$$

plus terms of order $|\mathbf{B} - \mathbf{B}_0|^2$. In (9), $D = \rho/\mu_0 = D(B_0, T)$ means the diffusivity of flux where $\rho(B_0, T)$ equals ρ_{TAFF} (3) or ρ_{FF} (section 3). Thus, in geometries where the current component $\mathbf{J}_\parallel$ parallel to $\mathbf{B}$ vanishes, ohmic resistivity is equivalent to a *linear diffusion of the flux lines*.

Since in the TAFF region $\rho = \rho_{TAFF} \propto \exp(-U/k_BT)$, one has for the thermally activated diffusion $D = \rho_{TAFF}/\mu_0 = D_0 \exp(-U/k_BT)$. For sufficiently large times, small specimens, and large T, any change of the applied magnetic field or current completely *penetrates* the HTSC, which then is in the *resistive* state. At lower T, such a change penetrates only into a thin *surface layer*, to the skin depth $\delta = (2D/\omega)$ or Campbell depth[92] $\lambda_C = (B^2/\mu_0\alpha_L)^{1/2}$ where α_L is the elastic pinning restoring force density on the FLL (Labusch parameter). The superconductor then behaves as if it were in the *Meissner* state, with almost complete expulsion of the applied field. In between these two limiting cases, the surface current penetrates more or less deeply and causes maximum dissipation when the skin depth coincides with a characteristic specimen dimension. The linear complex ac penetration depth λ_{ac} of a superconductor containing a FLL may be written as[21,93–94]

$$\lambda_{ac}(\omega) = \left[\lambda^2 + \lambda_C^2 \frac{1 - i/\omega\tau}{1 + i\omega\tau_0}\right]^{1/2} \tag{10}$$

The corresponding complex ac resistivity is

$$\rho_{ac}(\omega) = i\omega\mu_0\lambda^2 + \rho_{TAFF} \frac{1 + i\omega\tau}{1 + i\omega\tau_0}, \tag{11}$$

and the complex ac susceptibility of a slab of thickness d becomes

$$\mu(\omega) = \tanh(u)/u, \qquad u = d/2\lambda_{ac} \tag{12}$$

(Fig. 8). Here $\tau_0 = \eta/\alpha_L = \lambda_C^2/D_0$ is the relaxation time of an elastically pinned FLL and $\tau = \eta_{TAFF}/\alpha_L = B^2/\rho_{TAFF}\alpha_L = \lambda_C^2/D_{TAFF} = \tau_0 \exp(U/k_BT) \gg \tau_0$ is the creep time, i.e., the relaxation time for linear thermal depinning. Eqs. (10) to (12) apply also when the creep is caused by quantum tunneling of vortices out of the pinning wells[86–91] at T = 0. They describe the dissipation by flux-line motion only. Near T_c, losses by the normal conducting electrons may become important; this

has been accounted for by Coffey and Clem[93] within a two-fluid model. For concrete applications, λ_{ac}, $1/\lambda_{ac}$, λ_{ac}^2, ρ_{ac}, μ, etc., have to be decomposed into their real and imaginary parts.

Eqs. (10–12) show that for sufficiently low circular frequencies $\omega \ll 1/\tau$, one has flux diffusion with strongly temperature dependent diffusivity $D = D_0 \exp(-U/k_BT)$ and ohmic resistivity $\rho = \rho_{TAFF} = \rho_{FF} \exp(-U/k_BT)$. For recent experiments testing the above ac response see [95–96]. In the derivation of (10–12), after a sudden shift of the FLL, an exponential time decay of the elastic pinning force was assumed, $\alpha_L(t) \propto \exp(-t/\tau)$. Recent experiments observe an algebraic decay of $\alpha_L(t)$ in BSCCO ceramics[95] or an activation energy spectrum in BSCCO crystals[96].

9. DEPINNING LINES

The flux-diffusion picture explains a wide variety of experiments that all define an irreversibility line or depinning line $T_d(B)$, Fig. 7. The irreversibility line separates in the B-T plane the regions of irreversible (low B, T) and reversible (large B, T) magnetic behavior and can be explained by thermally activated depinning. Above this line the pins become ineffective and the vortices can move freely, giving rise to *reversible* magnetization curves, whereas below $T_d(B)$, hysteretic behavior is observed.

An interesting feature of the depinning line is that it depends on the size and shape of the specimen and on the time scale or frequency $\omega/2\pi$ of the experiment. This sometimes overlooked effect means that $T_d(B)$ is *not* a genuine intrinsic property of the material but originates from the *diffusive character* of the flux motion

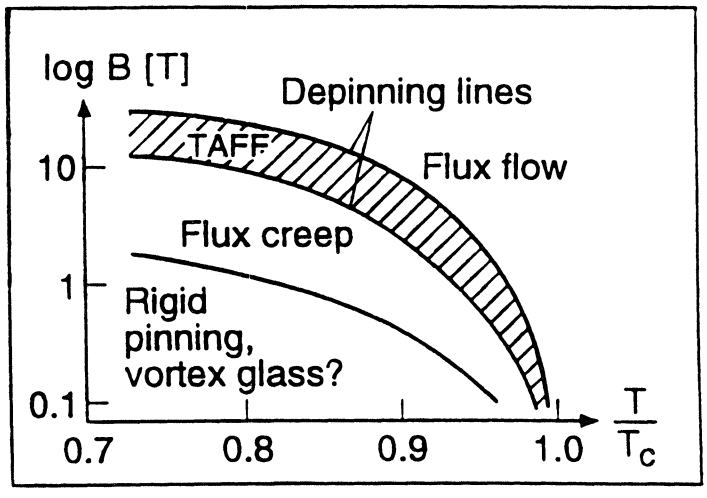

FIGURE 7 The depinning lines in the field-temperature plane separate the region of flux flow (complete depinning) from the region of flux creep (with slow logarithmic relaxation) and rigid pinning (with hysteretic behavior). At the depinning lines (dashed area) thermally assisted flux flow occurs (TAFF, flux diffusion, ohmic resistivity).

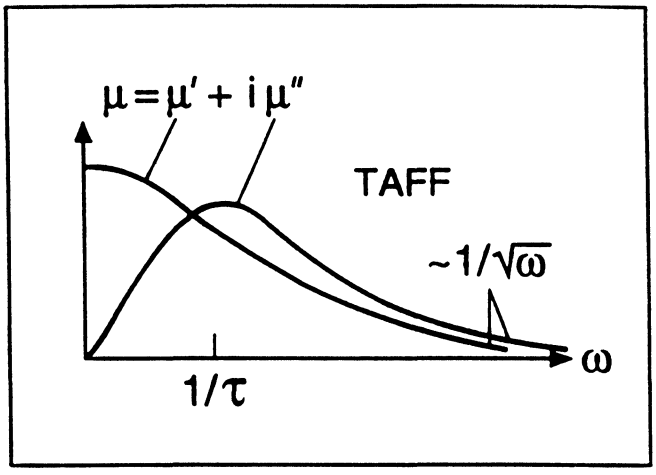

FIGURE 8 Complex a.c. susceptibility $\mu = \mu' + i\mu''$ (12) in the TAFF state, i.e., for $\omega \ll \tau^{-1}$ where $\rho \approx \rho_{TAFF}$ (11) and $\lambda_{ac} \approx \lambda_C/(i\omega\tau)^{1/2}$ (10), thus u in (12) becomes complex, $u = d/\lambda_{ac} = (1 + i)(\omega d^2/8D) = (1 + i)d/2\delta$ with $\delta = (2D/\omega)^{1/2}$ the skin depth.

and is *not* indicative of a sharp phase transition of any kind. Various experiments yield slightly different depinning lines:

(a) The irreversibility (hysteresis) in magnetization curves vanishes at $T_d(B)$. (b) A maximum in the imaginary part of the a.c. susceptibility (12) occurs at $T_d(B)$. (c) The ac penetration depth (10) measured by the screening of an ac field by a superconducting film between two coils[97] diverges at $T_d(B)$. (d) A sharp maximum in the attenuation of a vibrating HTSC in constant magnetic field and a corresponding reduction of the frequency enhancement is observed at $T_d(B)$[98–100]. Recently, even two such peaks were observed when the field was applied at an oblique angle with respect to a flat HTSC[101]. These peaks probably belong to different diffusion modes[102]. (e) The conduction noise in HTSC films at constant current density and at a given frequency exhibits a sharp peak as a function of B and T[103]. This noise is caused by depinning processes: each "plucking" of a vortex releases elastic energy of the FLL, which then relaxes viscously with an exponential time law. Below $T_d(B)$ the noise is small since only few depinning processes occur; at $T = T_d(B)$ the noise is maximum; and above $T_d(B)$ is decreases again since the viscous motion of the thermally depinned vortices is smooth. The depinning line shifts to larger T or B when a higher frequency band is selected.

(f) In the broadening of the resistive transition $\rho(T, B)$ in a magnetic field[64–70], the low-ρ tail originates from TAFF, but the main part of $\rho(T)$ (on a linear scale) may originate from thermal fluctuations of the order parameter near T_c, where superconducting islands nucleate and decay again. In BSCCO with its almost isolated CuO-layers, the very broad smearing of $\rho(T)$ may also be caused by the thermal nucleation of vortex-antivortex pairs in the layers, which leads to a Kosterlitz-Thouless-like transition with a power law current-voltage curve[104]. An interesting effect for B and J parallel to the ab-plane is that the resistivity does not

depend on the angle between B and J[105]. This has been explained by a small misalignment of B, which leads to the presence of point vortices in the layers that can move easily[106].

(g) An ultrasonic attenuation peak and sound velocity enhancement occurs at $T_d(B)$[107,108]. Ultrasound probes the FLL *far inside* a superconductor, whereas in the other methods (a)–(f), the FLL interacts with the outer world (the applied field or transport current) only near its *surface*, in a layer of thickness λ where shielding currents or transport surface currents exert forces on the vortex lines or on their end points (magnetic monopoles). The resulting compression or tilt deformation of the FLL then *diffuses* into the interior as described in [21, 53, 62, 94]. At lower T and at larger amplitude, this diffusion and the corresponding resistivity become *nonlinear*, i.e., they depend on the amplitude of the ac field or current.

10. CONCLUSION

For applications with large current densities or large magnetic fields, only superconductors of type II can be used. In these, magnetic flux lines (vortices) allow the magnetic field to penetrate partially, providing a larger upper critical field. It is, however, essential that the flux lines are pinned by material inhomogeneities such as structural defects or precipitates, otherwise they will move under the action of the Lorentz force. This flux motion dissipates energy and generates a voltage drop. Above a critical current density J_c the flux lines get unpinned. Strong pinning and large J_c, comparable to that in conventional superconductors like NbTi, in principle, can be achieved also in HTSC.

However, at the large temperature $T \approx 77$ K envisaged for applications, the flux lines in HTSC can *depin even at low current densities due to their thermal motion*. The small pinning energy of HTSC is due to the small vortex core radius (coherence length ξ) and to the high flexibility of the flux lines. Thermally activated pinning is particularly pronounced in the very anisotropic Bi- and Tl-based HTSC as soon as there is a magnetic field component perpendicular to the superconducting CuO planes. The activation energy for depinning of two-dimensional "pancake vortices" in the CuO planes is then very small, and even at T down to 4 K, flux creep occurs and the electric resistivity is not strictly zero. This undesired flux creep, in principle, may be reduced by using the less anisotropic YBCO, or by considering geometries where B is exactly along the CuO planes, or by synthesizing Bi and Tl HTSC with three or more CuO planes such that the pancake vortices become "thicker" and the pinning wells deeper.

REFERENCES

1. P.G. De Gennes, Superconductivity of Metals and Alloys (Benjamin, New York, 1966).
2. M. Tinkham, Introduction to Superconductivity (McGraw-Hill, New York, 1975).
3. A.A. Abrikosov, Fundamentals of the Theory of Metals (North Holland, Amsterdam, 1988).
4. A.A. Abrikosov, Zh. Eksper. Theor. Fiz. *32*, 1442 (1957); Soviet Phys.-J. Exp. Theor. Phys. *5*, 1174 (1957).
5. U. Essmann and H. Träuble, Phys. Lett. A *24*, 526 (1967).

6. U. Essmann and H. Träuble, Scientific American *224*, 75 (March 1971).
7. E.H. Brandt and U. Essmann, phys. stat. sol. (b) *144*, 13 (1987) (review).
8. J.G. Bednorz and K.A. Müller, Z. Phys. B *64*, 189 (1986).
9. M.K. Wu, J.R. Ashburn, C.J. Torng, P.H. Hor, R.L. Meng, L. Gao, Z.J. Huang, Y.Q. Wang, and C.W. Chu, Phys. Rev. Lett. *58*, 908 (1987).
10. P.L. Gammel, D.J. Bishop, G.J. Dolan, J.R. Kwo, C.A. Murray, L.F. Schneemeyer, and J.V. Waszczak, Phys. Rev. Lett. *59*, 2592 (1987).
11. L.Ya. Vinnikov, L.A. Gurevich, G.A. Yemel'chenko, and Yu.A. Ossipyan, Solid State Comm. *67*, 421 (1988).
12. J.R. Clem, J. Low Temp. Phys. *18*, 427 (1975).
13. E.H. Brandt, Phys. Rev. B *34*, 6514 (1986).
14. E.H. Brandt, J. Low Temp. Phys. *26*, 709; 735 (177); *28*, 263, 291 (1977).
15. K. Martinas, Phys. Lett. A *82*, 369 (1981); J. Kirschner and K. Martinas, J. Low Temp. Phys. *47*, 105 (1982).
16. V.G. Kogan, Phys. Rev. B *38*, 7049 (1988); Phys. Rev. B *24*, 1572 (1981); D.E. Farrell et al., Phys. Rev. Lett. *63*, 782 (1989); L. Fruchter et al., Physica C *160*, 185 (1989).
17. A.M. Grishin, A.Yu. Martynovich, and S.V. Yampol'skiĭ, Physica B *165 & 166*, 1103 (1990); A.I. Buzdin and A.Yu. Simonov, Sov. Phys. JETP Lett. *51*, 191 (1990); Physica B *165 & 166*, 1101 (1990); V.G. Kogan, Phys. Rev. Lett. *64*, 2192 (1990).
18. C.A. Bolle et al., Phys. Rev. Lett. *66*, 112 (1991); P.L. Gammel, D.J. Bishop, J.P. Rice, and D.M. Ginsberg, Phys. Rev. Lett. *68*, 3343 (1992).
19. E.H. Brandt, Physica B *165 & 166*, 1129 (1990); Physica B *169*, 91 (1991).
20. E.H. Brandt, Int. J. Mod. Phys. B. *5*, 751 (1991) (review).
21. E.H. Brandt, Physica C *195*, 1 (1992) (review).
22. A. Houghton, R.A. Pelcovits, and A. Sudbø, Phys. Rev. B *40*, 6763 (1989).
23. A. Sudbø and E.H. Brandt, Phys. Rev. B *43*, 10482 (1991); Phys. Rev. Lett. *66*, 1781 (1991); Phys. Rev. Lett. *68*, 1758 (1992); E. Sardella, Phys. Rev. B *45*, 3141 (1992).
24. E.H. Brandt and A. Sudbø, Physica C *180*, 426 (1991).
25. W.E. Lawrence and S. Doniach, Proc. 12th Internatl. Conf. of Low Temperature Physics LT12 (E. Kanda ed., Academic Press of Japan, Kyoto, 1971) p. 361.
26. L.N. Bulayevskiĭ, Int. J. Mod. Phys. B. *4*, 1849 (1990) (review).
27. M.V. Feigel'man, V.B. Geshkenbein, A.I. Larkin, Physica C *167*, 177 (1990); V.M. Vinokur, P.H. Kes, and A.E. Koshelev, Physica C *168*, 29 (1990).
28. L.N. Bulayevskiĭ, M. Ledvij, and V.G. Kogan, Phys. Rev. B *46*, 366 (1992).
29. D. Feinberg, Physica C *194*, 126 (1992).
30. E.H. Brandt, Phys. Rev. Lett. *66*, 3213 (1991).
31. J.R. Clem, Phys. Rev. B *43*, 7837 (1991); L.N. Bulayevskiĭ, S.V. Meshkov, and D. Feinberg, Phys. Rev. B *43*, 3728 (1991).
32. M. Tachiki and S. Takahashi, Solid State Commun. *70*, 291 (1989); Physica B *169*, 121 (1991);
33. L.I. Glazman and A.E. Koshelev, Phys. Rev. B *43*, 2835 (1991).
34. L.N. Bulayevskiĭ, M. Ledvij, and V.G. Kogan, Phys. Rev. Lett. *68*, 3773 (1992).
35. J. Bardeen and M.J. Stephen, Phys. Rev. *140*, A1197 (1965).
36. M. Tinkham, Phys. Rev. Lett. *13*, 804 (1964).
37. L.P. Gor'kov and N.B. Kopnin, Sov. Phys.-Uspechi *18*, 496 (1976).
38. A.I. Larkin and Yu.N. Ovchinnikov, in: Nonequilibrium Superconductivity, D.N. Langenberg and A.I. Larkin, eds. (Elsevier, Amsterdam, 1986), p. 493.
39. B.I. Ivlev and N.B. Kopnin, Phys. Rev. B *42*, 10052 (1990).
40. J.R. Clem and W.M. Coffey, Phys. Rev. B *42*, 6209 (1990).
41. Z. Hao and J.R. Clem, IEEE Trans. Magn. *27*, 1086 (1991).
42. J.R. Clem, in: Progress in Low Temperature Physics, R. Nikolski, ed. (World Scientific, Singapore, 1990), Vol. 25, p. 64.
43. P.W. Anderson, Phys. Rev. Lett. *9*, 309 (1962); P.W. Anderson and Y.B. Kim, Rev. Mod. Phys. *36*, 39 (1964).
44. C.P. Bean, Rev. Mod. Phys. *36*, 31 (1964); J. Appl. Phys. *41*, 2482 (1970).
45. M. Däumling and D.C. Larbalestier, Phys. Rev. B *40*, 9350 (1989); I. Kirschner, F. Balustri,

Gy. Kiss, I. Kovacs, L. Laszloffy, Gy. Remenyi and K. Saji, Zh. Exper. Theor. Fiz. *66*, 2141 (1974); Sov. Phys.-JETP *39*, 1054 (1974).
46. L.W. Connor and A.P. Malozemoff, Phys. Rev. B *43*, 402 (1991).
47. H. Theuss, A. Forkl, and H. Kronmüller, Physica C *190*, 345 (1992).
48. S. Senoussi, J. Physique J. Phys. III (Paris) *2*, 1041 (1992) (review); I. Kirschner, S. Leppävuori, R. Laiko, J. Altfeder and J. Dodony, Z. Physik B *85*, 175 (1991); I. Kirschner, S.Leppävuori, R. Laiko, A.D. Caplin, and J. Halasz, Cryogenics *31*, 33 (1991).
49. E.H. Brandt, Phys. Rev. B *46*, 8628 (1992).
50. M.R. Beasley, R. Labusch, and W.W. Webb, Phys. Rev. *181*, 682 (1969); see also: C. Rossel et al., Physica C *165*, 233 (1990); P. Berghuis and P.H. Kes, Physica B *165 & 166*, 1169 (1990); P. Svedlindh et al., Phys Rev. B *43*, 2735 (1991); M. Suenaga, A.K. Gosh, Y. Xu, and D.O. Welch, Phys. Rev. Lett. *66*, 177 (1991).
51. Y. Yeshurun and A.P. Malozemoff, Phys. Rev. Lett. *60*, 2202 (1988).
52. D. Dew-Hughes, Cryogenics *28*, 674 (1988).
53. P.H. Kes et al., Supercond. Sci. Technol. *1*, 242 (1989).
54. A.I. Larkin and Yu.N. Ovchinnikov, J. Low Temp. Phys. *43*, 109 (1979).
55. M.V. Feigel'man, V.B. Geshkenbein, A.I. Larkin, and V.M. Vinokur, Phys. Rev. Lett. *63*, 2303 (1989).
56. T. Nattermann, Phys. Rev. Lett. *64*, 2454 (1990); K.H. Fischer and T. Nattermann, Phys. Rev. B *43*, 10372 (1991).
57. V.M. Vinokur, M.V. Feigel'man, V.B. Geshkenbein, and A.I. Larkin, Phys. Rev. Lett. *65*, 259 (1990); M.V. Feigel'man and V.M. Vinokur, Phys. Rev. B *41*, 8986 (1990).
58. L. Civale, A.D. Marwick, T.K. Worthington, M.A. Kirk, J.R. Thompson, L. Krusin-Elbaum, Y. Sun, J.R. Clem, F. Holtzberg, Phys. Rev. Lett. *67*, 648 (1991).
59. W. Gerhäuser, G. Ries, H.W. Neumüller, W. Schmidt, O. Eibl, G. Saemann-Ischenko, and S. Klaumünzer, Phys. Rev. Lett. *68*, 879 (1992).
60. E.H. Brandt, Europhysics Letters *18*, 635 (1992); Phys. Rev. Lett. *69*, 1105 (1992).
61. D.R. Nelson and V.M. Vinokur, Phys. Rev. Lett. *68*, 2398 (1992).
62. E.H. Brandt, Z. Physik B *80*, 167 (1990).
63. A. Schmid and W. Hauger, J. Low Temp. Phys. *11*, 667 (1973).
64. T.T.M. Palstra, B. Battlogg, R.B. van Dover, L.F. Schneemeyer, and J.V. Waszczak, Phys. Rev. B *41*, 6621 (1990).
65. R.H. Koch et al. Phys. Rev. Lett. *63*, 1511 (1989).
66. Ph. Seng, R. Gross, U. Baier, M. Rupp, D. Koelle, R.P. Huebener, P. Schmitt, G. Saemann-Ischenko, and L. Schultz, Physica C *192*, 403 (1992).
67. J.C. van der Beek, G.J. Nieuwenhuys, P. Kes, H.G. Schnack, and R.P. Griessen, Physica C *197*, 320 (1992).
68. T.K. Worthington et al., Phys. Rev. B *43*, 10538 (1991).
69. T.K. Worthington, M.P.A. Fisher, D.A. Huse, J. Toner, A.D. Marwick, T. Zabel, C.A. Feild, and F. Holtzberg, Phys. Rev. B *46*, 11854 (1992).
70. P.L. Gammel, L.F. Schneemeyer, and D.J. Bishop, Phys. Rev. Lett. *66*, 953 (1991); N.-C. Yeh, et al., Phys. Rev. B. *45*, 5654 (1992); H. Safar et al., Phys. Rev. Lett. *68*, 2672 (1992);
71. S. Chakravarty, B.I. Ivlev, and Yu. N. Ovchinnikov, Phys. Rev. Lett. *64*, 3187 (1990); Phys. Rev. B *42*, 2143 (1990).
72. M.P.A. Fisher, Phys. Rev. Lett. *62*, 1415 (1989).
73. D.S. Fisher, M.P.A. Fisher, and D.A. Huse, Phys. Rev. B *43*, 130 (1991).
74. A.P. Malozemoff and M.P.A. Fisher, Phys. Rev. B *42*, 6784 (1990); M.V. Feigel'man, V.B. Geshkenbein, A.I. Larkin, and V.M. Vinokur, Phys. Rev. B *43*, 6263 (1991).
75. G. Blatter, M.V. Feigel'man, V.B. Geshkenbein, A.I. Larkin, and V.M. Vinokur, Review of Mod. Phys. (to be published, review paper).
76. A.A. Zhukov, Sol. St. Comm. *82*, 983 (1992).
77. H.G. Schnack, R. Griessen, J.G. Lensink, C.J. van der Beek, and P.H. Kes, Physica C *197*, 337 (1992).
78. E. Sandvold and C. Rossel, Physica C *190*, 309 (1992).
79. M.P. Maley and J.O. Willis, Phys. Rev. B *42*, 2639 (1990).

80. V.M. Vinokur, M.V. Feigel'man, and V.B. Geshkenbein, Phys. Rev. Lett. *67*, 915 (1991).
81. C.W. Hagen and R. Griessen, Phys. Rev. Lett. *62*, 2857 (1989); R. Griessen, Phys. Rev. Lett. *64*, 1674 (1990).
82. A. Gurevich, Phys. Rev. B *42*, 4857 (1990).
83. L. Niel and J. Evetts, Europhys. Lett. *15*, 453 (1991).
84. H. Theuss, T. Reininger, and H. Kronmüller, J. Appl. Phys. *72*, 1936 (1992).
85. J.G. Lensink, C.F.J. Flipse, J. Roobeek, R. Griessen, and B. Dam, Physica C *162–164*, 663 (1989); A.C. Mota, G. Juri, P. Visani, and A. Pollini, Physica C *162–164*, 1152 (1989); R. Griessen et al., Cryogenics *30*, 536 (1990); A. Fruchter et al., Phys. Rev. B *43*, 8709 (1991); M. Lairson et al., Phys. Rev. B *43*, 10405 (1991); A.C. Mota et al., Physica C *185–189*, 343 (1991).
86. R. Griessen, Physica C *172*, 441 (1991).
87. A.V. Mitin, Zh. Eksp. Teor. Fiz. *93*, 590 (1987) [Sov. Phys. JETP *66*, 335 (1987)].
88. B.I. Ivlev, Yu.N. Ovchinnikov, and R.S. Thompson, Phys. Rev. B *44*, 7023 (1991).
89. G. Blatter, V.B. Geshkenbein, and V.M. Vinokur, Phys. Rev. Lett. *66*, 3297 (1991).
90. R. Griessen, J.G. Lensink, and H.G. Schnack, Physica C *185–189*, 337 (1991).
91. G. Blatter and V.B. Geshkenbein, Phys. Rev. B *47*, 2725 (1993).
92. A.M. Campbell, J. Phys. C *4*, 3186 (1971); A.M. Campbell and J.E. Evetts, Adv. Phys. *21*, 199 (1972) (review).
93. M.W. Coffey and J.R. Clem, IEEE Trans. Magn. *27*, 2136 (1991) and erratum *27*, 4396 (1991); Phys. Rev. Lett. *67*, 386 (1991); Phys. Rev. B *45*, 9872 (1992).
94. E.H. Brandt, Phys. Rev. Lett. *67*, 2219 (1991); Physica C *185–189*, 270 (1991).
95. R. Behr, J. Kötzler, A. Spirgatis, and M. Ziese, Physica A *191*, 464 (1992).
96. D.G. Steel and J.M. Graybeal, Phys. Rev. B *45*, 12643 (1992).
97. A.F. Hebard, P.L. Gammel, C. Rice, and A. Levi, Phys. Rev. B *40*, 5243 (1989).
98. P. Esquinazi, J. Low Temp. Phys. *85*, 139 (1991) (review); Sol. St. Comm. *74*, 75 (1990).
99. J. Kober, A. Gupta, P. Esquinazi, H.F. Braun, and E.H. Brandt, Phys. Rev. Lett. *66*, 2507 (1991); A. Gupta, P. Esquinazi, and H.F. Braun, Phys. Rev. Lett. *63*, 1869 (1989); Physica B *165 & 166*, 1151 (1990).
100. P.L. Gammel, L.F. Schneemeyer, J.V. Waszczak, and D.J. Bishop, Phys. Rev. Lett. *61*, 1666 (1988); comment: E.H. Brandt, P. Esquinazi, and G. Weiss, Phys. Rev. Lett. *62*, 2330 (1989); reply: R.N. Kleiman, P.L. Gammel, L.F. Schneemeyer, J.V. Waszczak, and D.J. Bishop, Phys. Rev. Lett. *62*, 2331 (1989).
101. C. Durán, J. Yazyi, F. de la Cruz, D. Bishop, D.B. Mitzi, and A. Kapitulnik, Phys. Rev. B *44*, 7737 (1991); J. Yazyi, A. Arribére, C. Durán, F. de la Cruz, D.B. Mitzi, and A. Kapitulnik, Physica C *184*, 254 (1991); Y. Kopelevich, A. Gupta, P. Esquinazi, C.P. Heidmann, and H. Müller, Physica C *183*, 345 (1991).
102. E.H. Brandt, Phys. Rev. Lett. *68*, 3796 (1992).
103. A. Maeda, Y. Kato, H. Watanabe, I. Terasaki, and K. Uchinokura, Physica B *165 & 166*, 1363 (1990); E.S. Otabe, T. Matsushita, and K. Yamafuji, IEEE Trans. Magn. *27*, 1033 (1991).
104. Y. Ando, N. Motohira, K. Kitazawa, J. Takeya, and Shirabe Akita, Phys. Rev. Lett. *67*, 2737 (1991).
105. Y. Iye, S. Nakamura, and T. Tamegai, Physica C *159*, 443 (1989).
106. P.H. Kes, J. Aarts, V.M. Vinokur, and C.J. van der Beek, Phys. Rev. Lett. *64*, 1063 (1990).
107. J. Pankert, Physica C *168*, 335 (1990).
108. J. Pankert et al., Phys. Rev. Lett. *56*, 3052 (1990); P. Lemmens et al., Physica C *174*, 289 (1991); J. Pankert et al., Physica C *182*, 291 (1991); P. Lemmens, S. Ewert, and J. Pankert, Physica C *185*, 2271 (1991); M.J. Higgins, D.P. Goshorn, S. Bhattacharya, and D.C. Johnston, Phys. Rev. B *40*, 9393 (1989).